EFFICIENT ROTORCRAFT TRAJECTORY OPTIMIZATION USING COMPREHENSIVE VEHICLE MODELS BY IMPROVED SHOOTING METHODS

C.L. Bottasso, G. Maisano, F. Luraghi

Dipartimento di Ingegneria Aerospaziale,
Politecnico di Milano, Milano, Italy
carlo.bottasso@polimi.it, maisano@aero.polimi.it, luraghi@aero.polimi.it

Abstract

The present paper focuses on trajectory optimization problems for complex first-principle models of rotorcraft vehicles, accounting for the presence of slow and fast dynamic components in the solution. The trajectory optimal control problem is solved through a direct approach by means of a novel hybrid single-multiple shooting method. The capabilities of the proposed procedures are illustrated with the help of an application regarding the estimation of the H-V diagram of a tilt-rotor.

1 INTRODUCTION

The term *trajectory optimization* refers to the process of computing the optimal control inputs and the resulting response of a model of a vehicle, a rotorcraft in the present case, which minimize a cost function (or maximize an index of performance) while satisfying given constraints (which specify, for example, the vehicle flight envelope boundaries, and/or safety and procedural requirements for a maneuver of interest) [6, 7, 10, 11, 13]. Hence, one can usually give a precise definition of a maneuver by formulating an equivalent optimal control problem. The formulation of such a problem necessitates of a model of the vehicle system with its inputs, states and outputs, of a cost function and of a list of all constraints.

Clearly, the fidelity of the predictions made using this approach crucially hinges on the fidelity of the vehicle model. In fact, trajectories and performance limits predicted with oversimplified models might exhibit significant discrepancies with real flight data. Fidelity improvements may be obtained by considering a more sophisticated description of the vehicle; the current state-of-the-art calls for analysis tools based on comprehensive approaches [1, 4, 21, 27], which offer the ability to create hierarchical models of varying levels of fidelity of the various sub-systems of the vehicle.

Reference [13] illustrate a suite of trajectory optimization procedures which cater to vehicle models of varying complexity. Solution procedures for rotorcraft flight mechanics models have been previously described by Okuno and Kawachi [24], Carlson and Zhao [15], and Bottasso et al. [11, 12]. The extension of such procedures to handle fine-scale aero-servo-elastic comprehensive vehicle models have been first described by Bottasso et al. [8, 9].

In this work we focus on the direct multiple shooting approach to the solution of maneuver optimal control problems and on the so-called level 2 rotorcraft models, according to the classification of the different degrees of vehicle models' complexity into three levels proposed by Padfield [26].

As noted in Reference [22], these models are seldom used in the solution of optimization problems because it is often hard to provide the required accuracy within a reasonable computation time, while avoiding numerical instabilities due to the complex nonlinear rotor model. The reason for this is twofold: on the one hand, one needs to use a small integration time step length to correctly resolve the high frequency components of the solution within a given accuracy. On the other hand, one has to guarantee the continuity of the rotor states by imposing the proper gluing constraints. We have observed that the satisfaction of such constraints can be particularly difficult and usually ends up dominating the problem. This is not surprising, since the rotor generates most of the aerodynamic forces acting on the vehicle and even small variations in its states may imply large variations in the resulting forces, which hinders the satisfaction of the gluing constraints.

We have found that these problems can be alleviated by using multi-time scale arguments. In fact, level 2 models include both slow flight mechanics scales and faster ones, the latter being related to rotor degrees of freedom, including both structural (rigid and/or flexible) and aerodynamic states. To treat more

effectively this class of optimal control problems, we use multiple shooting on the slow scales, and single shooting on the faster ones; this avoids the enforcement of the multiple shooting gluing constraints for the faster scales, which improve efficiency and robustness of the direct methods when applied to complex vehicle models.

The paper is organized according to the following plan. After having more precisely defined the maneuver optimal control problem in Section 2, in Section 3 we review the mathematical formulation of direct shooting methods for their solution. In Section 4 we present a novel hybrid single-multiple shooting method specifically designed for dealing with the presence of different timescales in the model, whereas in Section 5 we describe an application of the proposed method to the estimation of the H-V diagram of the ERICA tilt-rotor [23]. Conclusions are given in Section 6.

2 THE MANEUVER OPTIMAL CONTROL PROBLEM

A maneuver can be defined as a finite-time transition between two trim conditions [18][1]. Clearly, given a start trim and an arrival trim, there is an infinite number of ways to transition between the two. A way to remove this arbitrariness is to formulate a maneuver as an optimal control problem [11, 7], where one minimizes a cost (time, altitude loss, control activity, fuel consumption, etc.) which in general is some given function of the vehicle states and control inputs. The solution of the optimization problem must satisfy the dynamic and kinematic equations of the vehicle, the initial and final conditions corresponding to the start and arrival trims, and all other equality and inequality constraints which need to be met in order to satisfy given performance and procedural requirements.

Consider a flight mechanics vehicle model $\mathcal{M}$, which includes structural and aerodynamic models of the vehicle components, possibly (but not necessarily) using a multibody approach [4]. The dynamics of model $\mathcal{M}$ can in general be described in terms of a set of non-linear index 1-3 differential algebraic equations written as

$$\boldsymbol{f}_{\mathrm{SD}}(\dot{\boldsymbol{x}}_{\mathrm{SD}}, \boldsymbol{x}_{\mathrm{SD}}, \boldsymbol{\lambda}, \boldsymbol{x}_{\mathrm{A}}, \boldsymbol{u}) = \boldsymbol{0}, \tag{1a}$$

$$\boldsymbol{c}(\boldsymbol{x}_{\mathrm{SD}}) = \boldsymbol{0}, \tag{1b}$$

$$\boldsymbol{M}\dot{\boldsymbol{x}}_{\mathrm{A}} + \boldsymbol{L}\boldsymbol{x}_{\mathrm{A}} - \boldsymbol{\tau}(\boldsymbol{x}_{\mathrm{SD}}, \boldsymbol{u}) = \boldsymbol{0}, \tag{1c}$$

where $\boldsymbol{x}_{\mathrm{SD}}$ are the structural dynamics states (including states which describe rigid and possibly flexible rotor(s), fuselage, engine, etc.), $\boldsymbol{\lambda}$ are constraint-enforcing Lagrange multipliers in a multibody vehicle model, $\boldsymbol{x}_{\mathrm{A}}$ are aerodynamic states (e.g. dynamic inflow variables), and $\boldsymbol{u}$ is the control input vector. Equations (1a) group together the equations of dynamic equilibrium and the kinematic equations. Equations (1b) represent mechanical joint constraint equations in a multibody vehicle model, while Eqs. (1c) are the aerodynamic state equations. Finally, the notation $\dot{(\cdot)} = \mathrm{d}(\cdot)/\mathrm{d}t$ indicates a derivative with respect to time t.

For the sake of simplicity, in the following we will consider that the Lagrange multipliers $\boldsymbol{\lambda}$ and redundant structural dynamics states can always be formally eliminated in favor of a minimal set of coordinates [19]. Therefore, the governing equations will be assumed to be of the ordinary differential type and will be simply expressed as

$$\boldsymbol{f}_{\mathrm{SD}}(\dot{\boldsymbol{x}}_{\mathrm{SD}}, \boldsymbol{x}_{\mathrm{SD}}, \boldsymbol{x}_{\mathrm{A}}, \boldsymbol{u}) = \boldsymbol{0}, \tag{2a}$$

$$\boldsymbol{M}\dot{\boldsymbol{x}}_{\mathrm{A}} + \boldsymbol{L}\boldsymbol{x}_{\mathrm{A}} - \boldsymbol{\tau}(\boldsymbol{x}_{\mathrm{SD}}, \boldsymbol{u}) = \boldsymbol{0}. \tag{2b}$$

When using quasi-steady aerodynamics, the aerodynamic model expressed by Eqs. (2b) and its associated aerodynamic states $\boldsymbol{x}_{\mathrm{A}}$ are of an algebraic nature. The numerical solution is in that case performed by eliminating the algebraic aerodynamic variables, usually through a fixed point iteration. Therefore, even in that case, we can consider an ODE model with no loss of generality.

It will be convenient to use a more synthetical form of the above equations in the following pages, and hence we will write the vehicle model as

$$\boldsymbol{f}(\dot{\boldsymbol{x}}, \boldsymbol{x}, \boldsymbol{u}) = \boldsymbol{0}, \tag{3a}$$

$$\boldsymbol{y} = \boldsymbol{h}(\boldsymbol{x}), \tag{3b}$$

where $\boldsymbol{x} = (\boldsymbol{x}_{\mathrm{SD}}^T, \boldsymbol{x}_{\mathrm{A}}^T)^T$ and $\boldsymbol{f}$ stacks together Eqs. (2a) and (2b). In addition, Eq. (3b) defines a vector of outputs $\boldsymbol{y}$. The outputs will typically represent some global vehicle states which describe its gross motion, such as position, orientation, linear and angular velocity of a vehicle-embedded frame with respect to an inertial frame of reference, or other quantities useful for formulating the maneuver optimal control problem.

Equations (3a) can be marched forward in time by providing a time history of control inputs $\boldsymbol{u}(t)$ and initial conditions on the states $\boldsymbol{x}(0) = \boldsymbol{x}_0$. In terms of its states, the response of system $\mathcal{M}$ to $\boldsymbol{u}(t)$ can be formally written as

$$\boldsymbol{x}(t) = \boldsymbol{\Phi}_{\boldsymbol{u}}(\boldsymbol{x}_0, t), \tag{4}$$

where $\boldsymbol{\Phi}_{(\cdot)}(\cdot,\cdot)$ is the state flow function. Accordingly, one obtains also the associated values of the outputs through (3b) as

$$\boldsymbol{y}(t) = \boldsymbol{h}(\boldsymbol{\Phi}_{\boldsymbol{u}}(\boldsymbol{x}_0, t)) = \boldsymbol{\Psi}_{\boldsymbol{u}}(\boldsymbol{y}_0, t), \tag{5}$$

[1] Although this is the only rigorous definition of a maneuver, in the context of the present work it will be more useful to use the term maneuver more loosely, and we will often consider the case of terminal conditions which are not trimmed.

where $\mathbf{\Psi}_{(\cdot)}(\cdot,\cdot)$ is the output flow function and $\boldsymbol{y}_0 = \boldsymbol{h}(\boldsymbol{x}_0)$.

The trajectory optimization problem is defined on the interval $\Omega = [0, T_f]$, $t \in \Omega$, where the final time T_f is typically unknown and must be determined as part of the solution to the problem. Specific events might be associated with unknown time instants T_e, $0 < T_e < T_f$, as for example the reaching of specific values of certain states, the jettisoning of part of the cargo, etc.

The maneuver optimal control problem (MOCP) consists in finding the control function $\boldsymbol{u}(t)$, and hence through (3a) the associated function $\boldsymbol{x}(t)$, which minimize the cost

$$\text{(6a)} \quad \min_{\boldsymbol{x},\boldsymbol{y},\boldsymbol{u},T_f} \quad J = \phi(\boldsymbol{y},t)\big|_0^{T_f} + \int_0^{T_f} L(\boldsymbol{y},\boldsymbol{u},\dot{\boldsymbol{u}},t)\,\mathrm{d}t,$$

$$\text{(6b)} \quad \text{s.t.:} \quad \boldsymbol{f}(\dot{\boldsymbol{x}},\boldsymbol{x},\boldsymbol{u}) = \boldsymbol{0},$$

$$\text{(6c)} \quad \boldsymbol{y} = \boldsymbol{h}(\boldsymbol{x}),$$

$$\text{(6d)} \quad \boldsymbol{g}(\boldsymbol{y},\boldsymbol{u},t,T_f) \leq \boldsymbol{0}.$$

The first term of Eqs. (6a) in the previous expression is a boundary or internal event term which accounts for values of the states at the initial and/or final instants and/or at the instant T_e corresponding to an event, while the second term is an integral cost term.

The minimizing solution must satisfy the vehicle equations of motion (6b), together with other constraints generically represented by Eqs. (6d), which can be boundary (initial and/or terminal) conditions on the states, bounds or any other kind of conditions.

2.1 Problem Complexity

In this section we introduce a measure C of the *complexity* of problem (6). A meaningful index which takes into account the underlying complexity of the problems to be solved is given by the expression

$$C_{\text{MOCP}} = \kappa\,\frac{T_f}{\tau}, \tag{7}$$

where κ is the number of unknown components in the problem, T_f is the length of the temporal domain and τ is the characteristic time length associated with the fastest solution scale component that one needs to resolve. In the context of the present discussion, κ is the number of states plus the number of inputs and outputs. For sophisticated models, the number of states is significantly larger than the number of inputs (which is usually very small for most vehicles) and of outputs (which is also typically a rather small number).

Problems of modest complexity use vehicle models with a small number of unknown quantities κ, and a solution is sought which captures only those components of the response which are slow compared to the overall duration (T_f/τ small). On the contrary, problems of high complexity use models with many unknown quantities (κ large, typically because of a large number of states) which capture fine scale response components, that are possibly very fast compared to the length of the temporal domain (T_f/τ large).

It is useful to introduce a complexity index reference value

$$C^*_{\text{MOCP}} = n^*_x \frac{T^*_f}{\tau^*_c}, \tag{8}$$

where $n^*_x = 12$ represents the number of standard flight mechanics states, $T^*_f = 10$ s is typical reference time duration for guidance problems [25] and finally $\tau^*_c = 0.1$ s is a typical characteristic timescale for flight mechanics problems. Hence, C^*_{MOCP} has a typical value of 1200. This is the complexity index of the simplest MOCP that one can solve.

This way we can define a more significant relative complexity index as

$$\overline{C}_{\text{MOCP}} = C_{\text{MOCP}}/C^*_{\text{MOCP}}. \tag{9}$$

The value of $\overline{C}_{\text{MOCP}}$ dictates the choice of the most suitable solution technique for the MOPC at hand, as depicted in Figure 1.

3 DIRECT SHOOTING METHODS

There are two principal approaches to the solution of trajectory optimization problem: indirect [3, 14, 17] and direct methods [5, 11, 12, 16]. Following [13], we prefer the direct approach even for the present paper. In fact, in the case of indirect methods one has first to derive the optimal control governing equations by using the calculus of variation, and then numerically solve the arising two-point boundary value problem. On the contrary, the direct approach does not require any manipulation of the equations of motion, as one first discretizes the problem by time stepping (using either a transcription or a shooting method [13]) and then solves the resulting Non-Linear Programming (NLP) problem [20] by a standard solver, such as SQP (Sequential Quadratic Programming).

Before describing the two methods used in this work, namely the direct single shooting (DSS) and the direct multiple shooting (DMS) methods, let us introduce some notation.

We consider a partition of the time domain Ω given by $0 = t_0 < t_1 < \ldots < \ldots < t_k < \ldots < t_N = T_f$ with $\Omega^k = [t_i, t_{i+1}]$, $k = (0, N-1)$, $i = k$, where each Ω^k is a shooting arc, or simply arc. Here and in the following, quantities associated with the generic vertex between segments i are indicated using the notation $(\cdot)_i$, while quantities associated with the generic segment k are labeled $(\cdot)^k$. In each shooting segment Ω^k, the controls are discretized as $\boldsymbol{u}^k(t) = \sum_{j=1}^{N^k_u} s_j(t)\boldsymbol{u}^k_j$ where $s_j(t)$ are basis functions, in particular cubic splines in the present implementation, and $\boldsymbol{u}^k_j$ are N^k_u

unknown discrete control values. If controls are discretized in the entire domain Ω, instead of in each arc, we use the notation $\boldsymbol{u}^{\Omega}$.

3.1 Direct Single Shooting

A single shooting approach is used whenever the dynamic system (3) is sufficiently stable. Starting from an initial condition, we march forward in time the equations of motion of the vehicle from 0 to T_f:

$$\boldsymbol{x}_{T_f} - \widehat{\boldsymbol{x}}_{T_f} = \boldsymbol{0}, \tag{10a}$$

$$\widehat{\boldsymbol{x}}_{T_f} = \widehat{\boldsymbol{\Phi}}_{\boldsymbol{u}^{\Omega}}(\boldsymbol{x}_0, T_f), \tag{10b}$$

where $\widehat{\boldsymbol{\Phi}}_{\boldsymbol{u}^{\Omega}(\boldsymbol{x}_0,T_f)}$ is the discrete counterpart of the flow function in Eqs.(4) and represents the numerical integration on the interval Ω. Here and in the following, we use the notation $\widehat{\boldsymbol{x}}$ to indicate the value of the states obtained by numerical integration in time.

In this case, the set of NLP variables (unknowns) is defined as:

$$\boldsymbol{z} = \left(\boldsymbol{u}^{\Omega}, \boldsymbol{x}_0, \boldsymbol{x}_{T_f}, T_f\right)^T, \tag{11}$$

i.e. they are defined as the discrete values of the controls within the entire time domain, the initial and final conditions on the states, and the final time. We remark that, in general, $\boldsymbol{x}_0$ and $\boldsymbol{x}_{T_f}$ will not be both unknown, since we typically use equation (6d) to define either the former or the latter.

Notice that with such an approach one does not need to partition the domain Ω, nor to impose any constraints on the states, as opposed to the case of the multiple shooting approach described below.

3.2 Direct Multiple Shooting

Multiple shooting is often advocated as a better, although somewhat empirical solution than single shooting when dealing with unstable systems, as for example when considering rotorcraft vehicles as in the present case. In fact, in optimal control problems, multiple shooting is the only way to avoid solution blow up caused by dramatic amplification of small perturbations [2].

The basic idea behind this approach is to break the time domain into multiple arcs Ω^k. The partitioning of Ω requires the introduction of constraints on the states, named gluing constraints, that ensure the continuity of their time history across the boundaries of the shooting segments. For the k-th arc $\Omega^k = [t_i, t_{i+1}]$ we have:

$$\boldsymbol{x}_{i+1} - \widehat{\boldsymbol{x}}_{i+1} = \boldsymbol{0}, \tag{12a}$$

$$\widehat{\boldsymbol{x}}_{i+1} = \widehat{\boldsymbol{\Phi}}_{\boldsymbol{u}^k}(\boldsymbol{x}_i, t_{i+1}), \tag{12b}$$

where now $\widehat{\boldsymbol{\Phi}}_{\boldsymbol{u}^k}$ is the flow function which brings the state vector from t_i to t_{i+1}. Equation (12a) translates the gluing constraints.

The set of NLP variables is defined as:

$$\boldsymbol{z} = (\boldsymbol{x}_{i=(0,N)}, \boldsymbol{u}^{k=(0,N-1)}_{j=(1,N^k_u)}, T_f)^T, \tag{13}$$

i.e. they are defined as the discrete values of the states at the interfaces between shooting segments, the discrete values of the controls within each segment, and the final time.

4 THE DIRECT SINGLE-MULTIPLE SHOOTING METHOD

In this section we describe the combined use of DMS and DSS methods for the solution of MOCPs.

As reported in Reference [22], level 2 fidelity models [26] are seldom used in the solution of optimization problems because it is often hard to provide the required accuracy within a reasonable computation time, while avoiding numerical instabilities due to the complex nonlinear rotor model.

The reason for this is twofold: on the one hand, one needs to use a small integration time step length to correctly resolve the high frequency components of the solution within a given accuracy. For rotorcraft models of the form (3a), this implies a potentially significant computational cost associated with the time-marching of the vehicle equations of motion (which represents the main contribution to the total cost of one iteration of the solution process). To obtain the total cost of one evaluation of the gluing constraints (12a), this time must be multiplied by the number of perturbations of the unknown states needed for the evaluation of the Jacobian matrix of the constraints. Clearly, as the number of model states increases, the computational cost grows accordingly.

On the other hand, one has to guarantee the continuity of the rotor states by imposing the proper gluing constraints (12a). We have observed that the satisfaction of such constraints can be particularly difficult and usually ends up dominating the problem. This is not surprising, since the rotor generates most of the aerodynamic forces acting on the vehicle and even small variations in its states may imply large variations in the resulting forces, which hinders the satisfaction of the gluing constraints.

We have found that these problems can be alleviated by using multi-time scale arguments. In fact, the rotor states (both structural and aerodynamic) are significantly faster than the flight mechanics ones[2].

[2]The flight mechanics states are here defined as those describing the gross rigid body motion of the vehicle, i.e. they represent the position, orientation, linear and angular velocities of a body-attached reference frame. The characteristic time length associated with this scales is of order $\mathcal{O}(1.0 - 0.1\mathrm{s})$.

Thus, since the multiple shooting treatment of these fast states is the main cause of the two aforementioned issues, i.e. raise in computational cost and difficulty in satisfying gluing constraints, one can think of treating slow and fast scales using different methods.

More specifically, we use a multiple shooting approach for the slow states, i.e. for every arc Ω^k we have:

$$\boldsymbol{x}_{\sim i+1} - \widehat{\boldsymbol{x}}_{\sim i+1} = \boldsymbol{0}, \tag{14a}$$

$$\widehat{\boldsymbol{x}}_{\sim i+1} = \widehat{\boldsymbol{\Phi}}_{\boldsymbol{u}^k}(\boldsymbol{x}_{\sim i}, \widehat{\boldsymbol{x}}_{\approx i}, t_{i+1}), \tag{14b}$$

where $\boldsymbol{x}_{\sim}$ and $\boldsymbol{x}_{\approx}$ are the states associated with slow and fast scales, respectively. This is crucial, since with single shooting small changes early in the trajectory can produce dramatic effects at the end of it [2]; hence, the multiple shooting treatment of slow scales avoids the blow up of the solution.

On the contrary, we treat the fast scales using a single shooting approach, as depicted in Figure 2:

$$\widehat{\boldsymbol{x}}_{\approx i+1} = \widehat{\boldsymbol{\Phi}}_{\boldsymbol{u}^k}(\boldsymbol{x}_{\sim i}, \widehat{\boldsymbol{x}}_{\approx i}, t_{i+1}). \tag{15a}$$

This does not compromise the robustness of the procedure, since fast scales will not diverge if slow ones do not; hence, the stabilizing effect produced by the multiple shooting treatment of slow scales is felt also at the level of the fast ones.

The set of NLP variables is defined as:

$$\boldsymbol{z} = (\boldsymbol{x}_{\sim i=(0,N)}, \boldsymbol{u}_{j=(1,N_u^k)}^{k=(0,N-1)}, T_f)^T. \tag{16}$$

5 ESTIMATION OF A TILTROTOR H-V DIAGRAM

In this section we describe the application of the proposed method to the estimation of the H-V diagram of a tilt-rotor. We consider a level 2 model of the ERICA vehicle [23] implemented in the general purpose flight simulator `FLIGHTLAB` [1]. The control inputs are defined as $\boldsymbol{u} = (\delta_{\text{coll}}, \delta_{\text{ped}}, \delta_{\text{lat}}, \delta_{\text{long}})^T$, where δ_{coll} is the collective stick deflection, δ_{ped} is the pedal deflection, δ_{lat} and δ_{long} are the lateral and longitudinal stick deflection, respectively. Results are presented in Figures 3 and 4.

In the following sections we describe the formulation of the maneuver optimal control problems that we consider here. Their relative complexity index $\overline{C}_{MOCP}$ varies between 12 and 50, depending on the maneuver duration.

5.1 Rejected take-off maneuver

In the rejected take-off (RTO) maneuver, the pilot, after an engine failure, aborts the take-off procedure to safely land. In this case one is interested in minimizing the region enclosed by the so-called *dead man's curve*.

The following constraints on the terminal condition specify the safety and procedural requirements for the maneuver:

$$\begin{aligned} H(T_f) &= 3.5\,\text{m}, \\ p(T_f) = q(T_f) = r(T_f) &= 0\,\text{deg/s}, \\ 0 \le V_Z(T_f) &\le 2.5\,\text{m/s}, \\ -1.0 \le \theta(T_f) &\le 10.0\,\text{deg}, \end{aligned}$$

where H is the height above the ground, V_Z is the linear velocity along the z-axis (pointing down) in a ground-attached inertial reference frame, θ is the pitch attitude, p, q, r are the roll, pitch, and yaw rate, respectively. Notice that for this maneuver the final height $H(T_f)$ is known, whereas the initial one $H(0)$ is an unknown of the problem.

The power loss after engine failure is simulated using the following law for the maximum available torque at the rotor shaft:

$$T_{\max}(t) = T_1 + (T_2 - T_1)e^{-t/\pi_1} + T_2 e^{-t/\pi_2}, \tag{18}$$

where T_1 is the hover torque required, T_2 is the one engine inoperative maximum take-off torque available at 100% rpm, while $\pi_1 = 1/9$ s and $\pi_2 = 8/9$ s are suitable time constants.

5.1.1 RTO maneuver: lower branch

In the case of the upper branch of the H-V diagram one is interested in *maximizing* the initial height from which the vehicle can safely land with one engine inoperative. The objective function which defines the maneuver takes the form

$$J_{\text{RTO}}^{\text{low}} = -H(0) + \frac{1}{T_f}\int_0^{T_f} \dot{\boldsymbol{u}}^T \boldsymbol{W} \dot{\boldsymbol{u}}\,\text{d}t, \tag{19}$$

where the integral term penalizes the control rates. The minus sign for the initial height $H(0)$ originates from the fact that the NLP problem solver used in this work implements a minimization procedure.

Figure 5 depicts some of the most relevant quantities for the RTO maneuver for the hover point. Notice that the control time history is such that at first it produces a reduction of rotor speed with the effect of reducing the final vertical velocity, thanks to the energy stored in the rotors. The computed maneuver duration is of about 5 s. The maximum starting height obtained is $H_{\max}^{\text{RTO low}}(0) = 14.44$ m.

5.1.2 RTO maneuver: upper branch.

In the case of the upper branch of the H-V diagram one is interested in *minimizing* the initial height from which the vehicle can safely land with one engine inoperative. Thus, in this case, the objective function

which defines the maneuver becomes

$$J^{\mathrm{up}}_{\mathrm{RTO}} = H(0) + \frac{1}{T_f}\int_0^{T_f} \dot{\boldsymbol{u}}^T \boldsymbol{W} \dot{\boldsymbol{u}}\,\mathrm{d}t, \tag{20}$$

where the first term now has a positive sign.

Figure 6 depicts some of the most relevant quantities for the RTO maneuver for the hover point. Notice that the maneuver can be divided into three different stages. During the first stage, after the engine failure, the rotor speed rapidly decreases, calling for a reduction of the collective input in order to increase the rotor rpm. At the same time, the longitudinal cyclic input makes the vehicle pitching down and accelerating forward. In the second stage, the rotor speed is stabilized around its upper bound, the collective input remains constant and the pitch angle reaches its lower bound. During the final stage, the collective input rapidly increases reaching its maximum allowed value, the vehicle pitches up and the vertical velocity increases up to the admitted value of $V_Z(T_f) = 2.5$ m/s, while the rotor speed decreases. In this case, the optimal initial height is $H^{\mathrm{RTO\,up}}_{\mathrm{min}}(0) = 42.1$ m.

Figure 7 illustrates the effects of using the nacelle tilt angle (DNAC) as an additional control. The performance is improved and the optimal initial height becomes $H^{\mathrm{RTO\,up}^*}_{\mathrm{min}}(0) = 27.93$ m. A comparison with the helicopter mode simulation shows that the maneuver duration is shorter and the maximum pitch angle is held for a shorter time due to the nacelle tilting, which ensures an appropriate acceleration.

5.2 Continued take-off maneuver

The continued take-off (CTO), or fly-away, maneuver has the following limitations:

$$\begin{aligned} U(t) &= \mathrm{const}, \\ p(T_f) = q(T_f) = r(T_f) &= 0\,\mathrm{deg/s}, \\ -10.0 \le V_Z(T_f) &\le -0.5\,\mathrm{m/s}, \\ -10.0 \le \theta(T_f) &\le 10.0\,\mathrm{deg}, \\ NR(T_f) &= 100.0\,\%, \end{aligned}$$

where U is the linear velocity along the x-axis in a ground-attached inertial reference frame and NR is the percentage of rotor nominal speed; along the entire maneuver

$$H(t) \ge 35\,\mathrm{ft}. \tag{22}$$

The cost function takes the same form of (20), i.e.

$$J_{\mathrm{CTO}} = H(0) + \frac{1}{T_f}\int_0^{T_f} \dot{\boldsymbol{u}}^T \boldsymbol{W} \dot{\boldsymbol{u}}\,\mathrm{d}t. \tag{23}$$

Observing Figure 9 we note that the optimized control time history is quite similar to that of the rejected take-off upper branch up to about 8 s, i.e. for the first two stages of the maneuver. During this lapse of time the goals are to recover the rotor speed and to stabilize the attitude and the descent velocity when the rotorcraft accelerates. The last stage is different and longer than in the rejected take-off case and it can be further subdivided: first the pitch angle increases to reduce the vertical velocity, then rotor speed, velocities and attitude are stabilized coherently with the final conditions. The optimal initial height is $H^{\mathrm{CTO}}_{\mathrm{min}} = 66.16$ m. Also in this case tilting the nacelles improves the performance and $H^{\mathrm{CTO}^*}_{\mathrm{min}} = 57.44$ m. The DNAC effects are less important than in the case of the RTO and the nacelle tilt angle returns to its initial value in order to increase the rate of climb. Figure10 shows a comparison between the maneuver in helicopter mode and the one with the use of nacelle tilting.

6 CONCLUSIONS

In this work we have presented a strategy for the efficient solution of rotorcraft trajectory optimization problems using comprehensive vehicle models based on the combined use of single and multiple shooting methods.

The proposed approach considers a subdivision of the model states based on timescale considerations. The slower rigid body states are treated with the multiple shooting method. This is crucial, since with single shooting small changes early in the trajectory can produce dramatic effects at the end of it; clearly, the problem is exacerbated when analyzing unstable systems, which is often the case when considering rotorcraft vehicles. Hence, the multiple shooting treatment of the flight mechanics scales avoids the blow up of the solution. On the other hand, the faster solution scales are treated using a single shooting strategy. This does not compromise the robustness of the procedure, since the rotor states will not diverge if the rigid body states do not blow up; hence, the stabilization produced by the multiple shooting treatment of the slower states is felt also at the level of the faster ones.

The combined single-multiple shooting approach based on a timescale separation argument leads to a robust and effective formulation for optimal control problems for vehicle models of significant complexity, which in general exhibits superior convergence and lower computational costs than either the single or the multiple shooting methods used individually.

References

[1] Advanced Rotorcraft Technology Inc., 1685 Plymouth Street, Suite 250, Mountain View, CA 94043, USA, `http://www.flightlab.com`.

[2] U.M. Ascher, R.M.M. Mattheij, and R.D. Russell. *Numerical solution of boundary value problems for ordinary differential equations*. Classics in Applied Mathematics, Philadelphia, 1995.

[3] R.L. Barron and C.M. Chick. Improved indirect method for air-vehicle trajectory optimization. *Journal of Guidance, Control and Dynamics*, 29(3):643–652, 2006.

[4] O.A. Bauchau, C.L. Bottasso, and Y.G. Nikishkov. Modeling rotorcraft dynamics with finite element multibody procedures. *Mathematics and Computer Modeling*, 33:1113–1137, 2001.

[5] H.G. Bock and K.J. Plitt. A multiple shooting algorithmfor direct solution of optimal control problems. In *Proceedings of the 9th IFAC World Congress*, pages 242–247, 1984.

[6] C.L. Bottasso. Solution procedures for maneuvering multibody dynamics problems for vehicle models of varying complexity. In *Multibody Dynamics*, volume 12, pages 57–79. Springer, Netherlands, 2008.

[7] C.L. Bottasso, C.-S. Chang, A. Croce, D. Leonello, and L. Riviello. Adaptive planning and tracking of trajectories for the simulation of maneuvers with multibody models. *Computer Methods in Applied Mechanics and Engineering*, 195(50), 2006.

[8] C.L. Bottasso, C.-S. Chang, A. Croce, D. Leonello, and L. Riviello. Adaptive planning and tracking of trajectories for the simulation of maneuvers with multibody models. *Computer Methods in Applied Mechanics and Engineering, Special Issue on Computational Multibody Dynamics*, 195:7052–7072, 2006.

[9] C.L. Bottasso, A. Croce, and D. Leonello. Multibody dynamics — Computational methods and applications. Computational Methods in Applied Sciences, chapter Neural-Augmented Planning and Tracking Pilots for Maneuvering Multibody Dynamics. Springer-Verlag, Dordrecht, The Netherlands, 2007. ISBN 1-4020-5683-4.

[10] C.L. Bottasso, A. Croce, D. Leonello, and L. Riviello. Optimization of critical trajectories for rotorcraft vehicles. *Journal of the American Helicopter Society*, 50:165–177, 2004.

[11] C.L. Bottasso, A. Croce, D. Leonello, and L. Riviello. Rotorcraft trajectory optimization with realizability considerations. *Journal of Aerospace Engineering*, 18(3):146–155, 2005.

[12] C.L. Bottasso, A. Croce, D. Leonello, and L. Riviello. Unsteady trim of maneuvering rotorcraft with comprehensive models. Rept. 05-02, Dipartimento Ingegneria Aerospazialem Politechico di Milano, Milan, Italy, 2005.

[13] C.L. Bottasso, G. Maisano, and F. Scorcelletti. Trajectory optimization procedures for rotorcraft vehicles, their software implementation and applicability to models of varying complexity. In *Proceedings of AHS 64th Annual Forum and Technology Display*, Montréal, Canada, April 29 – May 1 2008. Under review in Journal of the American Helicopter Society.

[14] A.E. Bryson and Y.C. Ho. *Applied Optimal Control*. Wiley, New York, 1975.

[15] E.B. Carlson and Y.J. Zhao. Optimal short takeoff of tiltrotor aircraft in one engine failure. *Journal of Aircraft*, 39:280–289, 2002.

[16] L. Cervantes and L.T. Biegler. *Optimization Strategies for Dynamic Systems, Encyclopedia of Optimization, Vol. 4*. C. Floudas, and P. Pardalos, Kluwer Academic, Norwell, MA.

[17] G. Fraser-Andrews. A multiple-shooting technique for optimal control. *Journal of Optimization Theory and Applications*, 102(2):299–313, 1999.

[18] E. Frazzoli. *Robust Hybrid Control for Autonomous Vehicle Motion Planning*. PhD thesis, Massachusetts Institute of Technology, Cambridge, MA, USA.

[19] M. Geradin and A. Cardona. *Flexible Multibody Dynamics, a Finite Element Approach*. John Wiley & Sons, New York, NY, 2000.

[20] P.E. Gill, W. Murray, and M.H. Wrightr. *Practical Optimization*. Academic Press, London and New York, 1981.

[21] W. Johnson. CAMRAD/JA: A comprehensive analytical model of rotorcraft aerodynamics and dynamics, Johnson Aeronautics version, Volume i: Theory manual. 1988.

[22] C.-J. Kim, S.K. Sung, S.H. Park, S.-N. Jung, and K. Yee. Selection of rotorcraft models for application to optimal control problems. *Journal of Guidance, Control, and Dynamics*, 31(5):1386–1399, 2008.

[23] F. Nannoni, G. Giancamilli, and M. Cicalè. ERICA: the european advanced tiltrotor. In *27th European Rotorcraft Forum*, September 11–14 2001.

[24] Y. Okuno and K. Kawachi. Optimal takeoff procedures for a transport category tiltrotor. *Journal of Aircraft*, 30:291–292, 1993.

[25] G. Padfield and M. White. Measuring simulation fidelity through an adaptive pilot model. *Aerosp. Sci. Technol*, 9:400–408, 2005.

[26] G.D. Padfield. *Helicopter Flight Dynamics*. Blackwell Science, Boston, MA, 1996.

[27] M. Rutkowski, G.C. Ruzicka, R.A. Ormiston, H. Saberi, and Y. Jung. Comprehensive aeromechanics analysis of complex rotorcraft using 2GCHAS. *Journal of the American Helicopter Society*, 40:3–17, 1995.

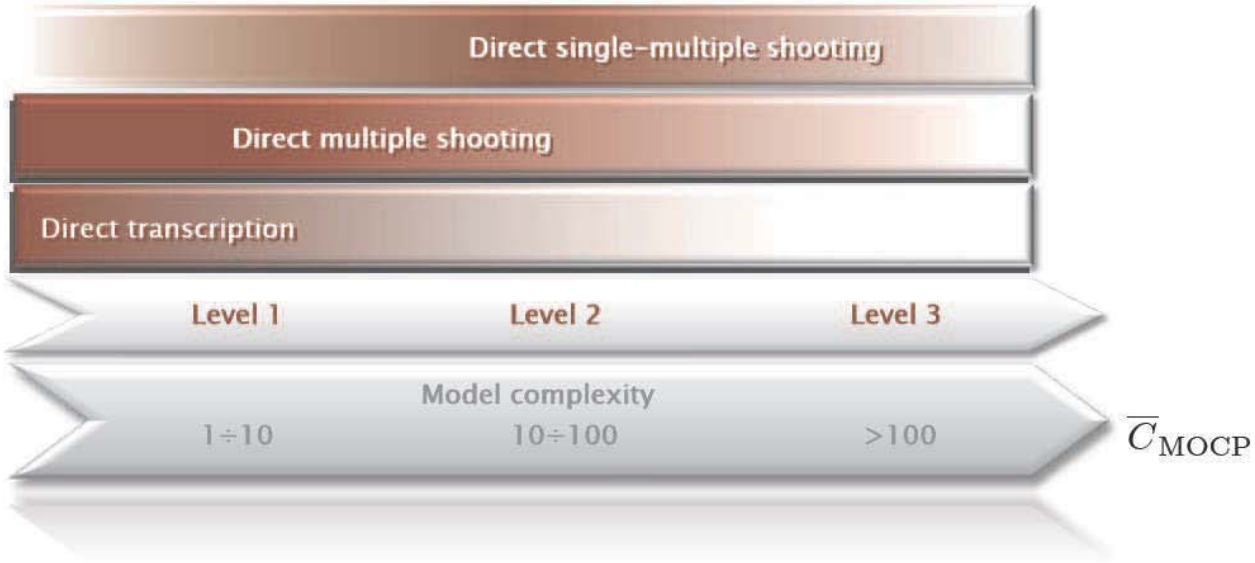

Figure 1: Preferred methods for vehicle models of increasing complexity.

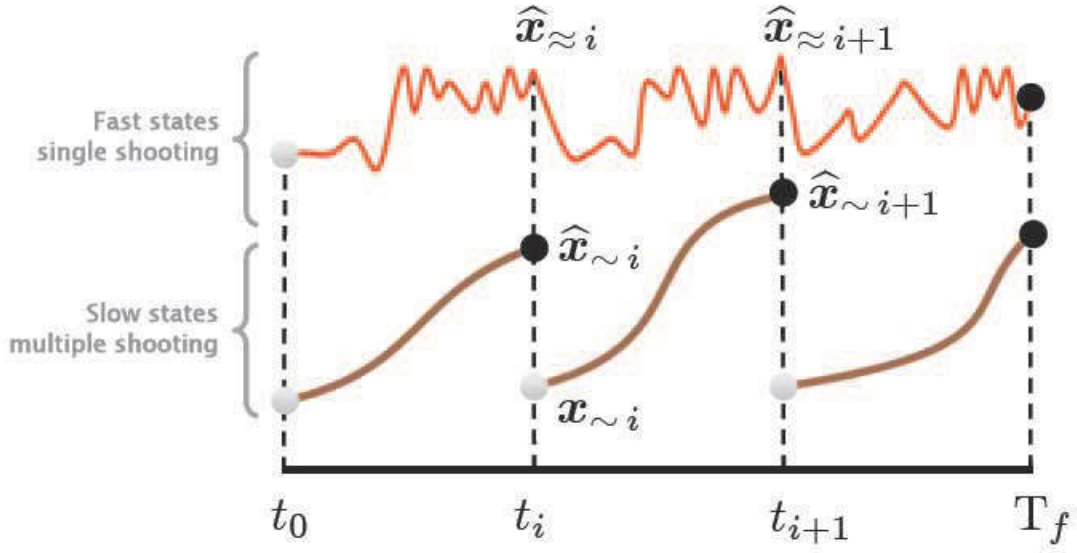

Figure 2: Hybrid single-multiple shooting approach.

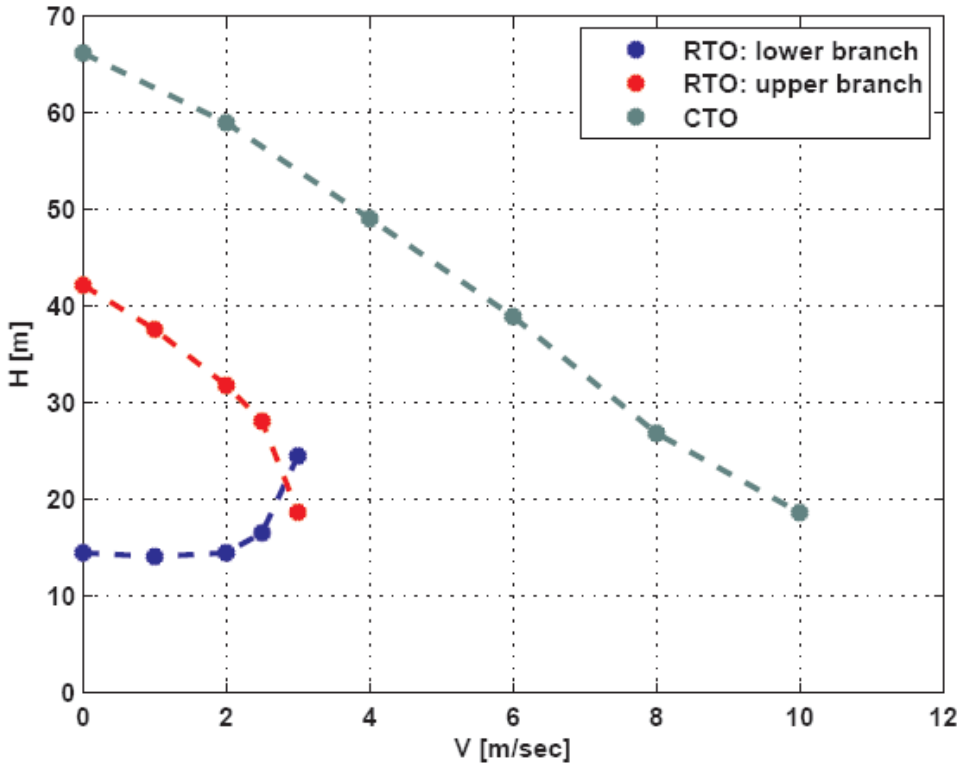

Figure 3: H-V diagram.

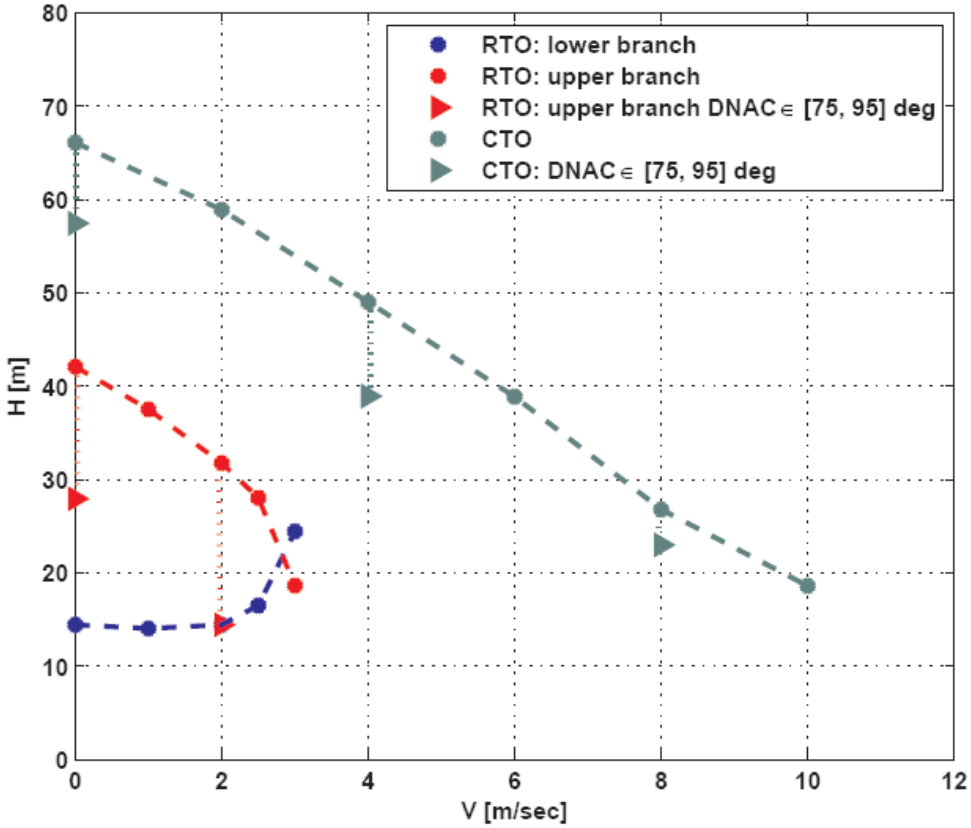

Figure 4: H-V diagram: effects of using the nacelle tilt angle (DNAC) as an additional control.

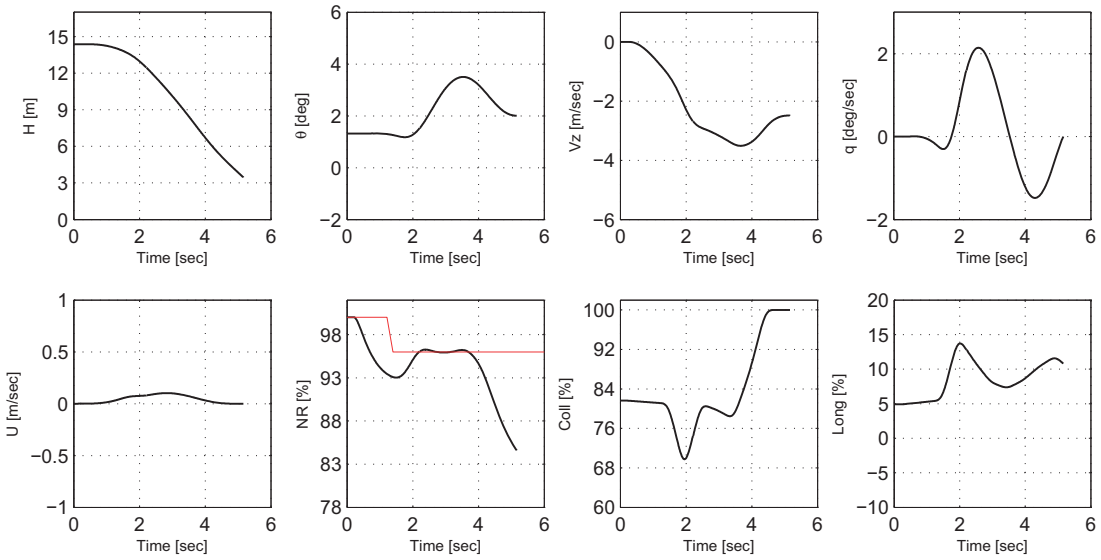

Figure 5: RTO maneuver: lower branch, hover point. Up, from left to right: height above the ground, pitch attitude (with bounds in red), vertical velocity (inertial frame, z-axis pointing down), pitch rate. Bottom, from left to right: longitudinal velocity with respect to the ground, rotor rpm (with bounds in red), collective stick deflection, longitudinal stick deflection.

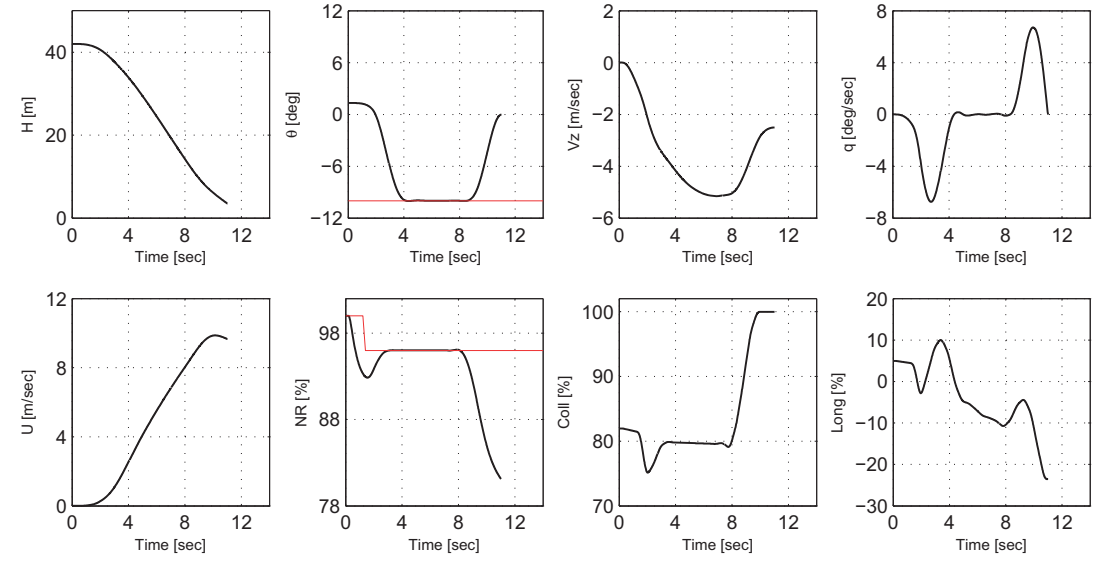

Figure 6: RTO maneuver: upper branch, hover point. Up, from left to right: height above the ground, pitch attitude, vertical velocity (inertial frame, z-axis pointing down), pitch rate. Bottom, from left to right: longitudinal velocity (inertial frame, x-axis pointing forward), rotor rpm (with bounds in red), collective stick deflection, longitudinal stick deflection.

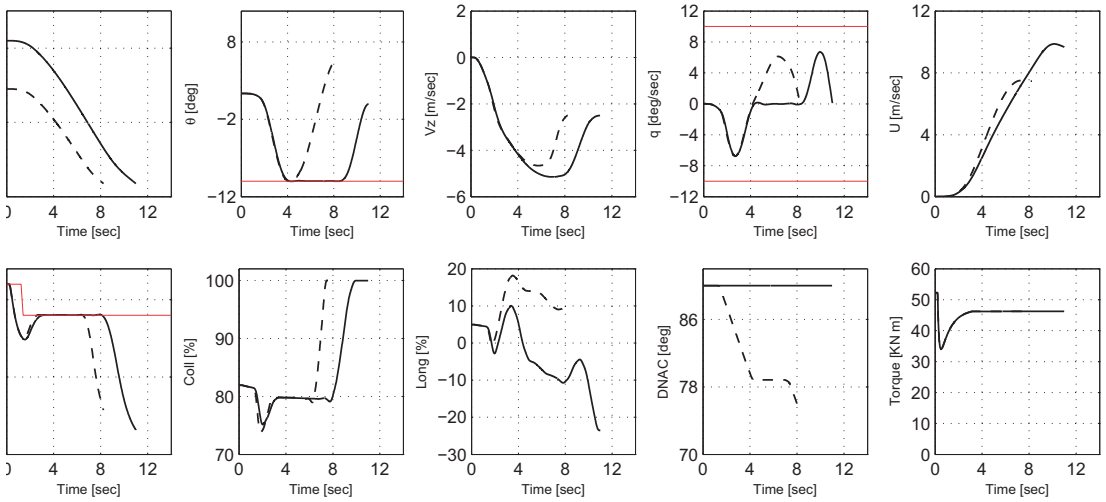

Figure 7: RTO maneuver: upper branch, hover point. Effects of using the nacelle tilt angle (DNAC) as an additional control. Helicopter mode (solid line) and DNAC effects (dashed line). Up, from left to right: height above the ground, pitch attitude (with bounds in red), vertical velocity (inertial frame, z-axis pointing down), pitch rate (with bounds in red), longitudinal velocity (inertial frame, x-axis pointing forward). Bottom, from left to right: rotor rpm (with bounds in red), collective stick deflection, longitudinal stick deflection, nacelle tilt angle, torque.

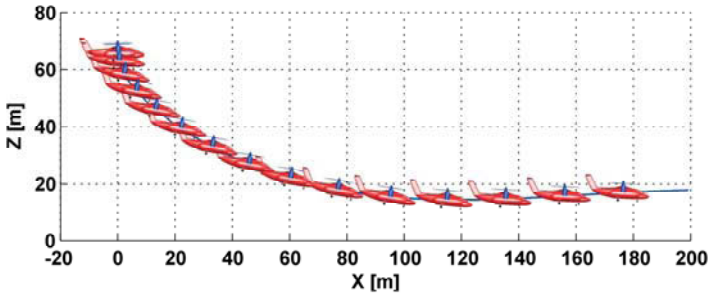

Figure 8: Hover point CTO: trajectory. In red some bounds.

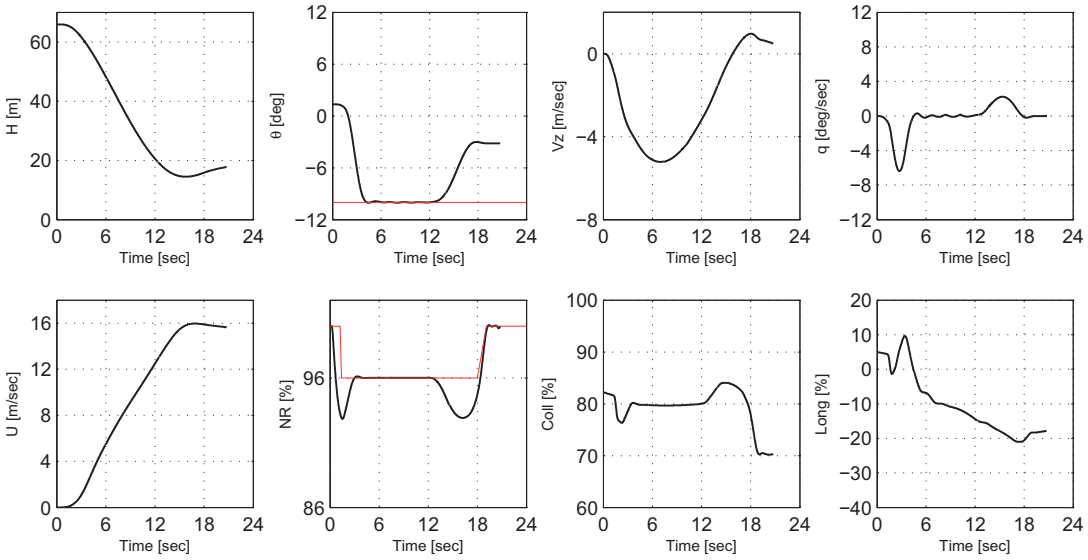

Figure 9: CTO maneuver: hover point. Up, from left to right: height above the ground, pitch attitude (with bounds in red), vertical velocity (inertial frame, z-axis pointing down), pitch rate. Bottom, from left to right: longitudinal velocity (inertial frame, x-axis pointing forward), rotor rpm (with bounds in red), collective stick deflection, longitudinal stick deflection.

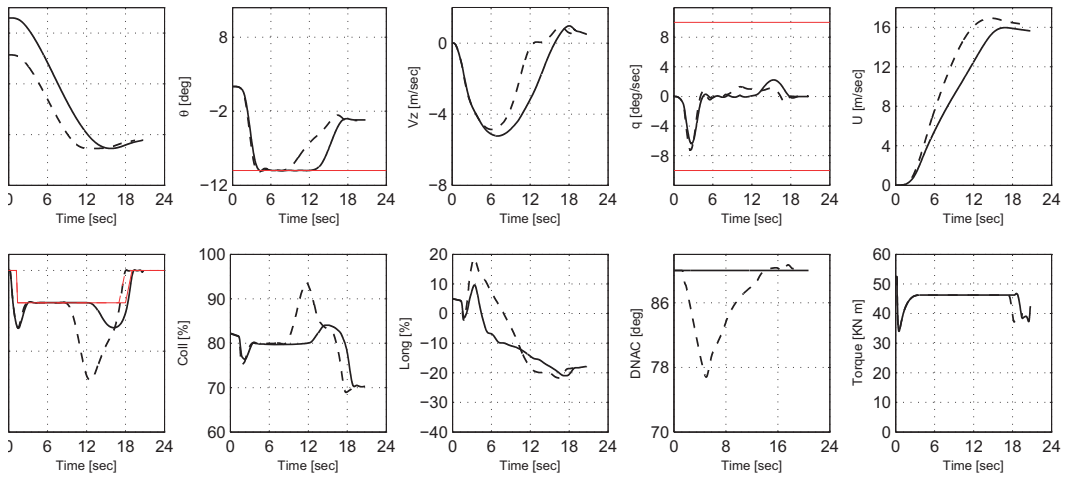

Figure 10: CTO maneuver: hover point. Effects of using the nacelle tilt angle (DNAC) as an additional control. Helicopter mode (solid line) and DNAC effects (dashed line). Up, from left to right: height above the ground, pitch attitude (with bounds in red), vertical velocity (inertial frame, z-axis pointing down), pitch rate (with bounds in red), longitudinal velocity (inertial frame, x-axis pointing forward). Bottom, from left to right: rotor rpm (with bounds in red), collective stick deflection, longitudinal stick deflection, nacelle tilt angle, torque.